Supplementary Information for

Structural basis of calmodulin modulation of the rod cyclic nucleotide-gated channel

Diane C.A. Barret [1]*, Dina Schuster [1, 2, 3]*, Matthew J. Rodrigues [1], Alexander Leitner [2], Paola Picotti [2], Gebhard F.X. Schertler [1], U. Benjamin Kaupp [4, 5], Volodymyr M. Korkhov[1, 3], and Jacopo Marino [1 #]

[1] Laboratory of Biomolecular Research, Paul Scherrer Institute, Villigen, Switzerland.

[2] Institute of Molecular Systems Biology, Department of Biology, ETH Zürich, Zürich, Switzerland.

[3] Institute of Molecular Biology and Biophysics, ETH Zürich, Zürich, Switzerland.

[4] Life and Medical Sciences Institute LIMES, University of Bonn, Bonn, Germany.

[5] Max Planck Institute for Multidisciplinary Sciences, Göttingen, Germany

[*] Contributed equally

[#] Correspondence to: jacopo.marino@psi.ch

This PDF file includes:

Materials and Methods

Sample preparation and cryo-electron microscopy

The rod CNG channel was purified from commercially available bovine rod outer segment membranes (Invision BioResources) as described previously [1], with subsaturating concentration of 50 µM cGMP (Sigma Aldrich) present in all buffers. The CNG channel concentration was 0.3 mg/ml. Bovine brain calmodulin (Sigma Aldrich) was added at a final concentration of 10 µM to the purified CNG channel. The protein sample was incubated on ice between 20 min and 1 h before the preparation of cryo-grids. R2/2 carbon grids (Quantifoil® holey carbon films with 2 nm continuous carbon on top) were glow discharged in a PELCO easiGlow (Ted Pella) glow discharge cleaning system, for 15 s at 10 mAmp in air. A small amount of protein sample (3.5 µl) was applied to glow-discharged grids and blotted using Vitrobot Mark IV (Thermo Fisher Scientific). Grids were blotted using the following parameters: blot force 1, blotting for 2 seconds, 100% humidity at 4°C. Grids were immediately plunged into liquid ethane and stored into liquid nitrogen until cryo-EM data collection. Grids were imaged in a Titan Krios G4 microscope operated at 300 kV (Thermo Fisher Scientific), equipped with a Gatan K3 direct electron detector and a Gatan Quantum-LS GIF, at ScopeM ETH Zurich. Imaging was performed in super-resolution mode at the calibrated pixel size of 0.51 Å, with a total dose of 62 $e^{-}/Å^{2}$ and defocus range of -0.8 to -2.2 µm.

Single-particle processing and model building

A total of 98,428 movies were collected over two microscope sessions using the same acquisition parameters. Movies were imported into cryoSPARC v.3.3.1 [2], motion corrected, dose weighted and binned by two to a pixel size of 1.02 Å/pixel. The contrast-transfer function (CTF) was estimated using Patch CTF from cryoSPARC. A small fraction of micrographs was discarded as they had CTF resolution above 6 Å, and displayed values outside the average (defocus, phase shift, relative ice thickness, astigmatism and total full-frame motion). On the remaining micrographs, particles were picked using the gaussian blob-picker embedded in cryoSPARC. Particles were subjected to several rounds of two-dimensional (2D) classification and manual selection of 2D classes. Particles belonging to selected 2D classes from all datasets were merged into a set of 279,337 particles. After ab-initio with two classes and zero similarity, one class displayed slightly more detailed secondary structure elements, and this volume was therefore used as input together with the final set of 279,337 particles for a non-uniform refinement job in cryoSPARC, which yielded a map at 2.81 Å. A further local CTF refinement job using as input the volume, particles, and mask of the non-uniform refinement yielded a map at 2.76 Å that was used for model building of the full channel except the coiled-coil region that is only partially visible in this density map. The structure of the bovine rod CNG channel (PDB: 7O4H) was used as a starting model, and the structure was modeled in Coot [3]. Overall, the map is of excellent quality and allowed to model many side chains. Various parts of the channel had to be adjusted manually, and the transmembrane region of CNGB1 (S1- S4 segments) was built de novo.

3D-variability analysis was set to two modes, and performed using the final stack of 279,337 particles and a mask that included the coiled-coil region, but excluded the micelle around the channel. The 3D variability display job was set in simple mode, with output volumes downsized to a box size of 220 and filter at 6 Å, which allowed to obtain the movies shown as Suppl. Video 1 and Suppl. Video 2. To separate particles according to the orientation of the coiled-coil region, the output particle component 1 of the 3D-variability job was connected to a 3D variability display job in intermediate output mode, from which particles were subdivided according to the 20 frames of the variability job. Particles belonging to frames 0-6, where the coiled-coil region is most visible and the connection between the CNGA1 coiled-coil and the

CNGB1 D-helix is visible, were used as input for a local refinement job together with a mask that included only the coiled-coil region. The volume obtained displayed a resolution of 4.66 Å and was used to rigid-body fit the three helices of the CNGA1 coiled-coil, the CNGB1 D-helix, and the C-terminal lobe of CaM, which were obtained by model prediction in AlphaFold2 [4]. This model was manually adjusted in Coot and no side chains were modeled. It remained difficult, at this resolution, to determine the precise orientation of calmodulin. However, after our model was deposited at the PDB, the NMR structure of CaM bound to the CaM2 became available and we noticed that our structure fits well to the NMR structure **(SI Appendix, Fig. S10)**. The final atomic model thus consists of information merged from the two density maps, the one obtained after local CTF refinement (deposited under EMBD: EMD-16311), and the one obtained after local refinement of the coiled-coil region (deposited under EMBD: EMD-16313). The atomic model is deposited under accession number PDB: 8BX7. The channel model consists of the following amino acid residues: CNGA1 K151-G615, P618-T670, and for CNGB1 Q760-L862, V871-K1203, and G1237-L1265. Model validation was performed in MolProbity [5], while refinement was performed in PHENIX [6].

Structure analysis

Structures were superimposed in ChimeraX. Distances between Cα atoms were measured in PyMol and ChimeraX, and figures were prepared in ChimeraX [7] and PyMOL[8]. Pore size measurements were obtained by using Hole [9].

LiP-MS sample preparation

Rod outer segment membranes were prepared from commercially available dark-adapted bovine retinae (W. L: Lawson Company, USA) as previously described [10]. Membrane pellets were further resuspended in 100 mM HEPES-KOH pH 7.4, 150 mM KCl, 1 mM $MgCl_2$ using a dounce homogenizer (20 strokes). The protein concentration was determined using the Pierce™ BCA protein assay kit. The membrane suspensions were diluted to a concentration of 2 mg/mL, additionally adding $CaCl_2$ to a final concentration of 1 mM. 36 aliquots à 50 µL were prepared in PCR strips. Calmodulin from bovine testes (Sigma Aldrich) was resuspended in 50 mM HEPES-NaOH pH 7.5, 150 mM NaCl to a concentration of 4 mg/mL and serially diluted under addition of $CaCl_2$ to a final concentration of 1 mM. Five bovine retinas were sufficient for one LiP-MS experiment (28 titration LiP samples and 8 tryptic control samples).

Limited proteolysis

All experiments were conducted in quadruplicates. Limited proteolysis was performed for all calmodulin concentrations, whereas tryptic controls were prepared for only the lowest (0 µg) and highest (3 µg) concentrations. Serial dilutions of calmodulin (final amounts per sample (in 57 µL): 0 µg, 0.01 µg, 0.1 µg, 0.5 µg, 1 µg, 2 µg, 3 µg) were added to the respective membrane suspension aliquots and incubated for 10 minutes at 25°C. 1 µg of proteinase K (from *Tritirachium album;* Sigma Aldrich) or the same volume of water (tryptic controls) was added to the samples and incubated for 5 minutes at 25°C. The samples were incubated at 99°C for 5 minutes, followed by a cooling step at 4°C for an additional 5 minutes. An equal volume of 10% sodium deoxycholate was added to all samples (5% final sodium deoxycholate concentration).

Tryptic digest

The samples were transferred to a 96-well plate, where disulfide bonds were reduced by incubation with 5 mM tris(2-carboxyethyl)phosphine at 37°C for 40 minutes, using slight agitation. Free cysteines were alkylated for 30 minutes with 40 mM iodoacetamide in the dark at room temperature with slight agitation. The samples were diluted to a sodium deoxycholate concentration of 1% with 100 mM ammonium bicarbonate. The samples were digested with Lys-C (1 µg) and trypsin (1 µg) overnight at 37°C with slight agitation. The digestion was stopped by adding formic acid to a concentration of 2%, which precipitated sodium deoxycholate.

C18 clean-up

Precipitated sodium deoxycholate was removed by filtration (96-well Corning® 2 µm PVDF plate) and peptides were desalted using a 96-well MacroSpin plate (The Nest Group). Peptides were eluted with 50% acetonitrile, 0.1% formic acid and dried in a vacuum centrifuge. The dried peptides were stored at -20°C until further use.

LC-MS/MS

Prior to measurement, the samples were reconstituted in 22 µL 5% acetonitrile, 0.1% formic acid with addition of iRT peptides (Biognosys). An aliquot of each replicate of a condition was used to prepare pooled samples for the generation of spectral libraries. 1 µL of each sample was injected onto an Easy nLC 1200 nanoflow LC system and separated on a heated (50°C), in-house packed C18 column with 3 µm beads (Dr. Maisch ProntoSIL-200 C18-AQ) using a linear gradient from 3-35% B (Eluent A: 0.1% formic acid, Eluent B: 95% acetonitrile, 0.1% formic acid) over 120 minutes at a flowrate of 300 nL/min. Pooled samples were measured with data dependent acquisition (DDA), whereas the rest of the samples was measured with data independent acquisition (DIA) on an Orbitrap Exploris™ 480 mass spectrometer. DDA method: For DDA measurements, the Orbitrap MS1 resolution was set to 120,000 with a scan range between 350-1150 m/z. Normalized AGC target was set to 200% and RF lens to 50%. Charge states 2-6 were selected for higher energy collisional dissociation (HCD) fragmentation. The exclusion time was set to 20 s and the number of subsequent dependent scans was set to 20. MS2 Orbitrap resolution was set to 30,000 and the HCD collision energy to 30%.

DIA method: For DIA measurements the Orbitrap resolution was set to 120,000, AGC target was set to 200%. The scan range was between 350-1150 m/z, RF lens percentage was set to 50%. Cycle time was 3 seconds. The DIA method consisted of 41 variable width windows with 1 m/z overlap. The HCD collision energy for all scans was set to 30%, Orbitrap MS2 resolution was set to 30,000.

The limited proteolysis-coupled mass spectrometry data has been deposited to the ProteomeXchange Consortium via the PRIDE partner repository [11] with the dataset identifier PXD038768.

Data analysis

The raw data was analyzed using Spectronaut version 15 [12]. A contaminant FASTA file was prepared from the commonly found contaminants listed by MaxQuant [13]. Single hits were excluded and 5 amino acids were set as the minimum peptide length. Data was median normalized in Spectronaut and imputation was disabled. The pooled samples were used for library generation. Tryptic controls were searched separate from limited proteolysis samples. For the analysis of limited proteolysis samples trypsin was selected as the protease and the specificity was changed to semi-specific. For quantification, peptides were grouped by their modified sequence.

The results were exported from Spectronaut and imported into R (v. 4.1.1) for further data analysis. The data was analyzed using the R packages tidyverse (v. 1.3.1) [14], data.table (v. 1.14.2) [15] and protti (v. 0.5.0) [16]. Briefly, using an implementation of the drc R package [17], four parameter dose-response curves were fit onto measured intensities of all modified peptide sequences identified from either CNGA1 or CNGB1. Peptides with a Pearson correlation r of > 0.85 were considered to be significantly changing. The changing peptides were mapped onto the protein structure with protti and visualized in PyMOL (v. 2.5.3) (*The PyMOL Molecular Graphics System, Version 2.5.3, Schrödinger, LLC.*, n.d.). More details on the data analysis can be found on GitHub (https://github.com/dschust-r/CNG_LiP_MS) and on PRIDE (PXD038768).

XL-MS chemical crosslinking

20 µL of the CNG channel at a concentration of 1.2 mg/mL purified from bovine rod outer segments as previously described [1] were crosslinked with calmodulin at a 1:2 molar ratio. Briefly, 1 µL of calmodulin from bovine testes (Sigma Aldrich; 4 mg/mL in 50 mM HEPES-NaOH pH 7.5, 150 mM NaCl) was added to the CNG channel and incubated at 25°C for 10 minutes at 300 rpm. Primary amines were crosslinked with 1 mM disuccinimidyl suberate (1:1 ratio of DSS-d0 and DSS-d12; Creative Molecules; 25 mM stock in dimethyl formamide) at 25°C for 1 hour at 300 rpm. The crosslinking reaction was quenched by addition of ammonium bicarbonate to a final concentration of 50 mM. The sample was dried in a vacuum centrifuge.

Tryptic digest

The sample was resuspended in 50 µL 8 M urea. Disulfide bonds were reduced with 2.5 mM tris(2-carboxyethyl) phosphine over 30 minutes at 37°C. Free cysteines were alkylated with 5 mM iodoacetamide at room temperature, in the dark for 30 minutes. Proteins were digested in two steps: First, 0.3 µg (1:100 protein: protease) of Lys-C were added to the sample and incubated at 37°C for 2 hours at 800 rpm. Then the sample was diluted with 320 µL 50 mM ammonium bicarbonate and further digested by adding a 1:50 ratio of trypsin (0.6 µg) and incubating at 37°C, 800 rpm overnight. The next day the digest was stopped by adding formic acid to a concentration of 2%.

C18 clean-up

Peptides were desalted via solid-phase extraction (MicroSpin Columns 5-60 µg capacity, The Nest Group), eluted with 50 % acetonitrile, 0.1% formic acid and dried in a vacuum centrifuge. The sample was resuspended in 30% acetonitrile, 0.1% trifluoroacetic acid and fractionated using size-exclusion chromatography (Superdex 30 Increase column, 300 x 3.2 mm; GE

Healthcare) at a flow rate of 50 µL/min in 30% acetonitrile, 0.1% trifluoroacetic acid. Four fractions were collected and dried in a vacuum centrifuge.

LC-MS/MS

The samples were resuspended in 15 µL 5% acetonitrile, 0.1% formic acid and 6 µL were injected onto an Easy nLC-1200 HPLC system (Thermo Scientific) coupled to an Orbitrap Fusion™ Lumos™ mass spectrometer. Peptides were separated with a linear gradient from 11-40% B (Eluent A: 2% acetonitrile, 0.15% formic acid; B: 80% acetonitrile, 0.15% formic acid) over 60 min, at a flow rate of 300 nL/min on an Acclaim PepMap RSLC C18 column (250 x 75 µm, Thermo Scientific). The samples were measured in duplicates with data dependent acquisition. Cycle time was set to 3 seconds with dynamic exclusion for 30 seconds. RF lens percentage was set to 40%, AGC target to 200,000 and the maximum injection time was 50 ms. MS1 Orbitrap resolution was set to 120,000, charge states between +3 and +7 were selected and fragmented in a linear ion trap with collision-induced dissociation. Collision energy was set to 35%, the activation time was 10 ms. Ion trap scan rate was set to rapid and the maximum injection time was 100 ms. The fragmented mass range was set to 350-1500 m/z. The crosslinking mass spectrometry data have been deposited to the ProteomeXchange Consortium via the PRIDE partner repository [11] with the dataset identifier PXD038640.

Data analysis

For the generation of a FASTA file with all present protein sequences, the raw files were analyzed with Spectromine version 3 (Biognosys) and searched against the bovine proteome (reviewed and unreviewed sequences downloaded from UniProt [18]) and a contaminants database (generated from MaxQuant [13]). Proteins with more than 5% of the label-free quantity of the target proteins were retained in the FASTA file used for the crosslinking analysis. All subsequent analyses were carried out with xQuest v. 2.1.5 [19]. The sequences in the FASTA file were reversed and shuffled for the generation of a decoy database. Trypsin was chosen as the digestion enzyme, a maximum number of 2 missed cleavages was tolerated. Carbamidomethylation on cysteines was included as a fixed modification and oxidation of methionine residues was included as a variable modification. The peptide length was set to 4-40 amino acids, MS1 error tolerance was ± 15 ppm, MS2 tolerance was ± 0.2 Da. Crosslinked residues were lysines and the protein N-termini.

The data was further analyzed using xQuest/xProphet viewer. Crosslinked peptides were analyzed and filtered separately, depending on the type of crosslink. All peptides were filtered with a mass tolerance window of ± 5 ppm with a minimum number of 3 matched ions and a delta score < 0.9. To achieve a false discovery rate of < 5%, the target and decoy hits at different Id scores were compared for heteromeric and homomeric crosslinks. Heteromeric crosslinks were additionally required to be detected at least 3 times, with an Id score ≥ 30. All spectra were checked manually for TIC ≥ 0.1 and at least 3 sequential or 4 bond breakages within each peptide.

Data visualization of mass-spec results

Heteromeric and homomeric crosslinks were visualized with XiNet [20], PyXlinkViewer [21] and PyMOL (v. 2.5.3) [8].

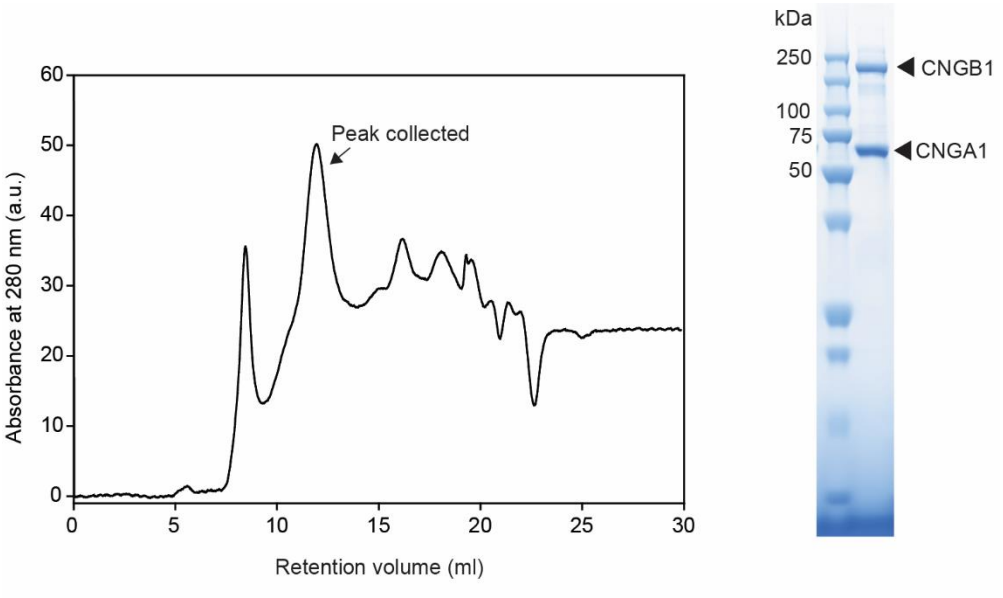

Figure S1. **Size exclusion profile of the purified bovine rod CNG channel and relative SDS-page gel.** The CNG channel was purified following the procedure described in [1]. The fraction containing the CNG channel is indicated (peak collected), which was concentrated for the preparation of cryo-EM grids. a.u., arbitrary units.

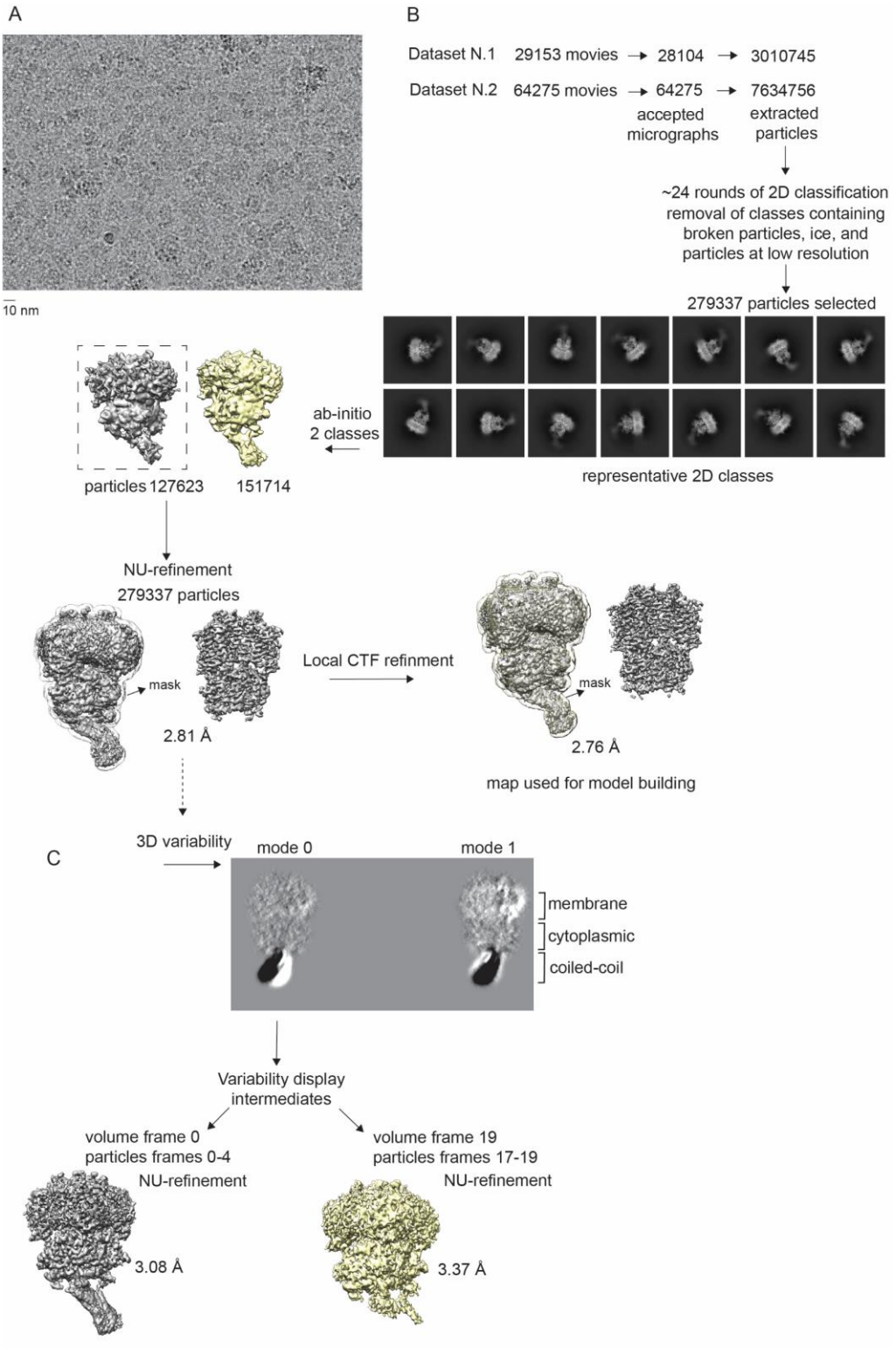

Figure S2. Cryo-EM single-particle analysis. A) Representative micrograph from one of the three datasets. **B)** Summary of the single-particle pipeline used to obtain the final density map used for model building. **C)** Summary of the output of the 3D-variability analysis.

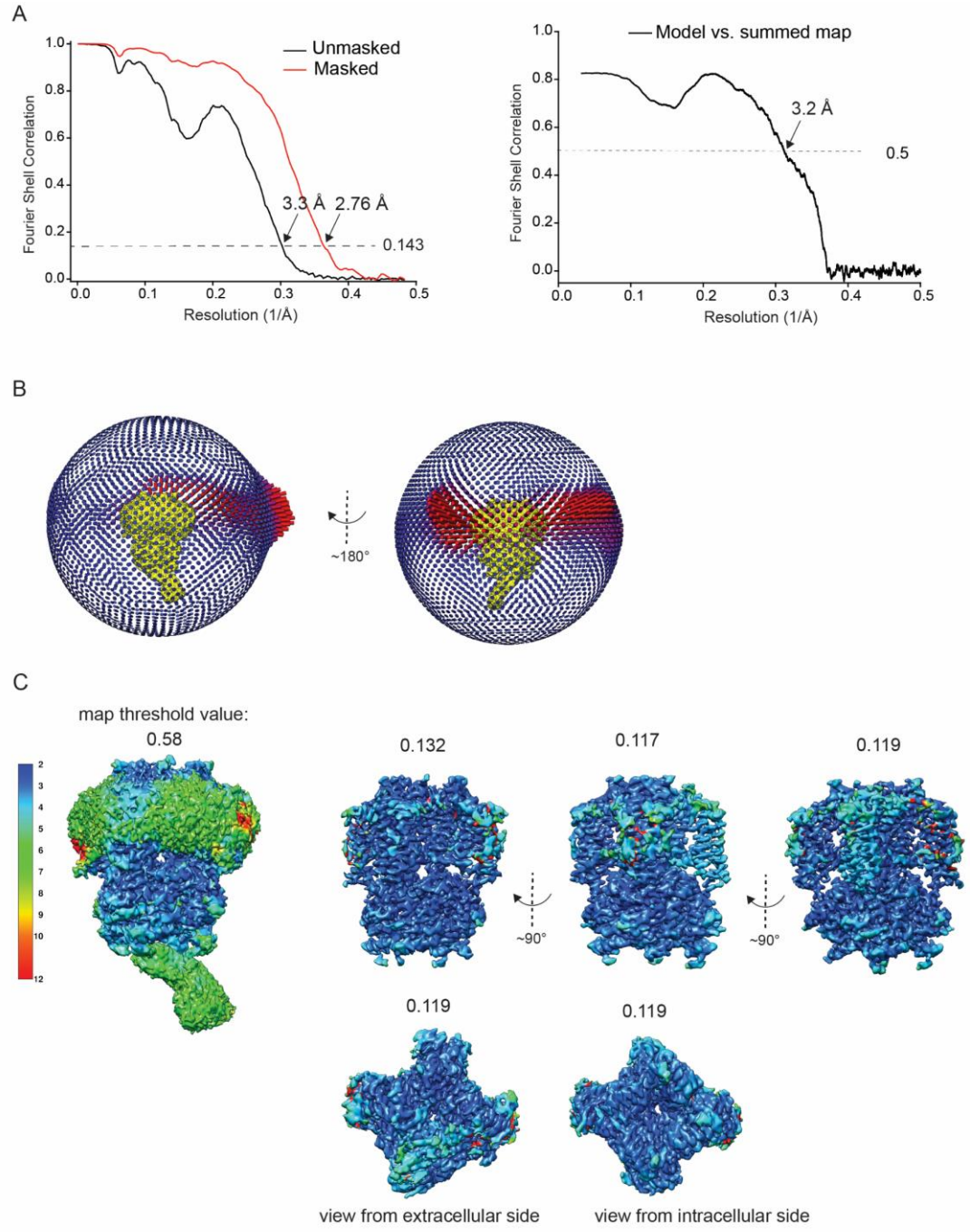

Figure S3. FSC curves and details of the density map. A) On the left, gold-standard FSC curves of the final 3D reconstruction, and on the right, FSC curve for validation of map and model. **B)** Euler angle distribution of the set of particles that contribute to the final density map. **C)** Local resolution of the final density map shown at different threshold values (as displayed in Chimera) and different orientations.

Data collection and processing	
Magnification	165,000
Voltage (kV)	300
Electron exposure (e^-/Å²)	62
Defocus range	-0.8 to -2.2
Pixel size (super resolution)	0.51
Bin factor during processing	2
Symmetry	C1
Initial particle images (no.)	10645501
Final particle images (no.)	279337
FSC threshold	0.143
Map resolution estimate (Å)	2.76
Refinement	
Model resolution (Å)	3.2 (Å)
FSC threshold	0.5
Map sharpening *B* factor	none
Model composition	
Atoms (non-hydrogen)	15637
Residues	2059
Ligands	0
Bonds (RMSD):	
Length (Å)	0.003
Angles (°)	0.652
Validation	
MolProbity score	2.11
Clash score	10.63
Ramachadran Plot (%):	
Outliers	0.05
Allowed	5.39
Favored	94.56

SI Table 1. Cryo-EM data collection, refinement and validation statistics.

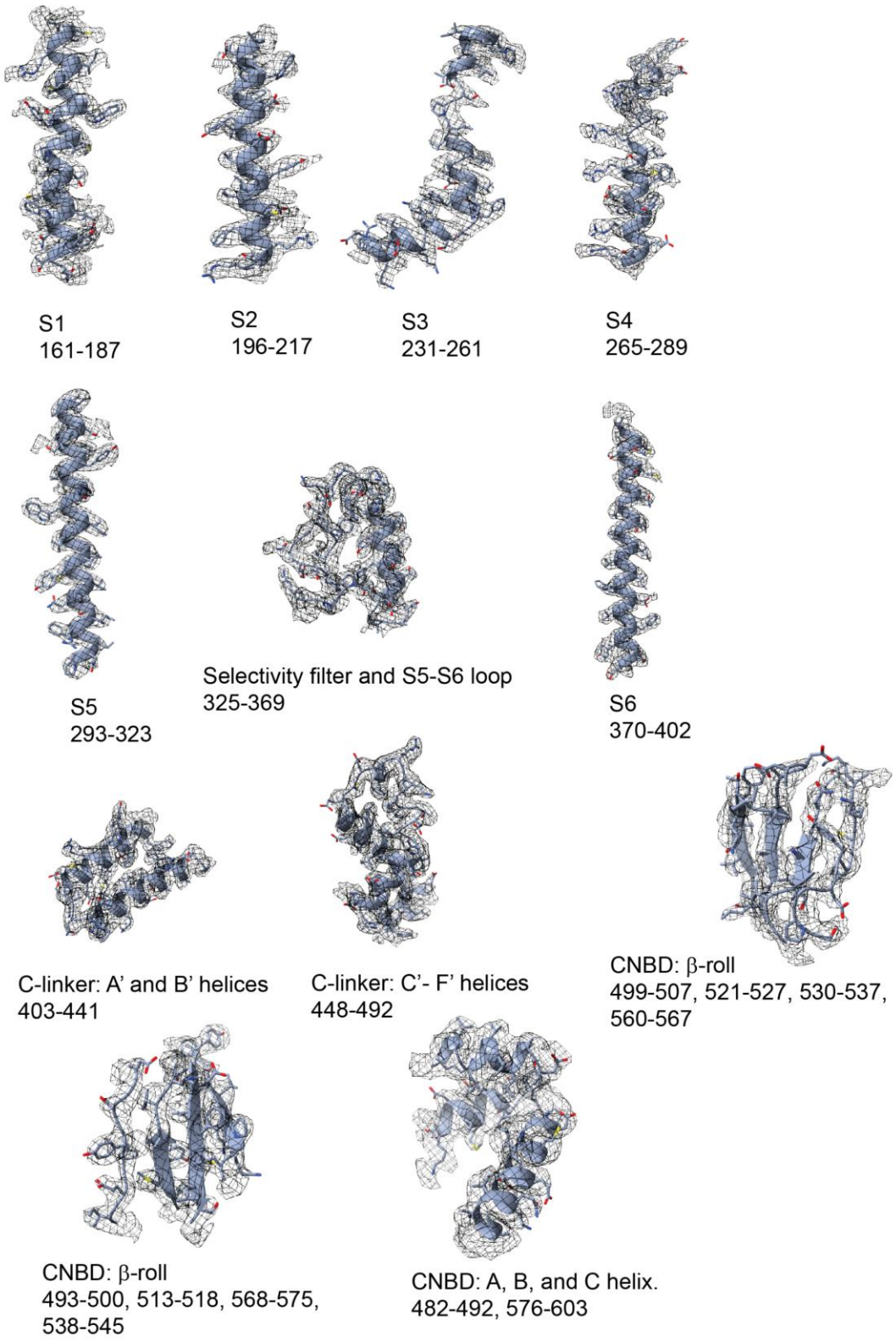

Figure S4. Cryo-EM density map of CNGA1 and relative atomic model of selected regions. The density map relative to one of the CNGA1 subunits (chain C) is shown. The map was contoured at threshold values ranging between 0.187 and 0.118 in ChimeraX.

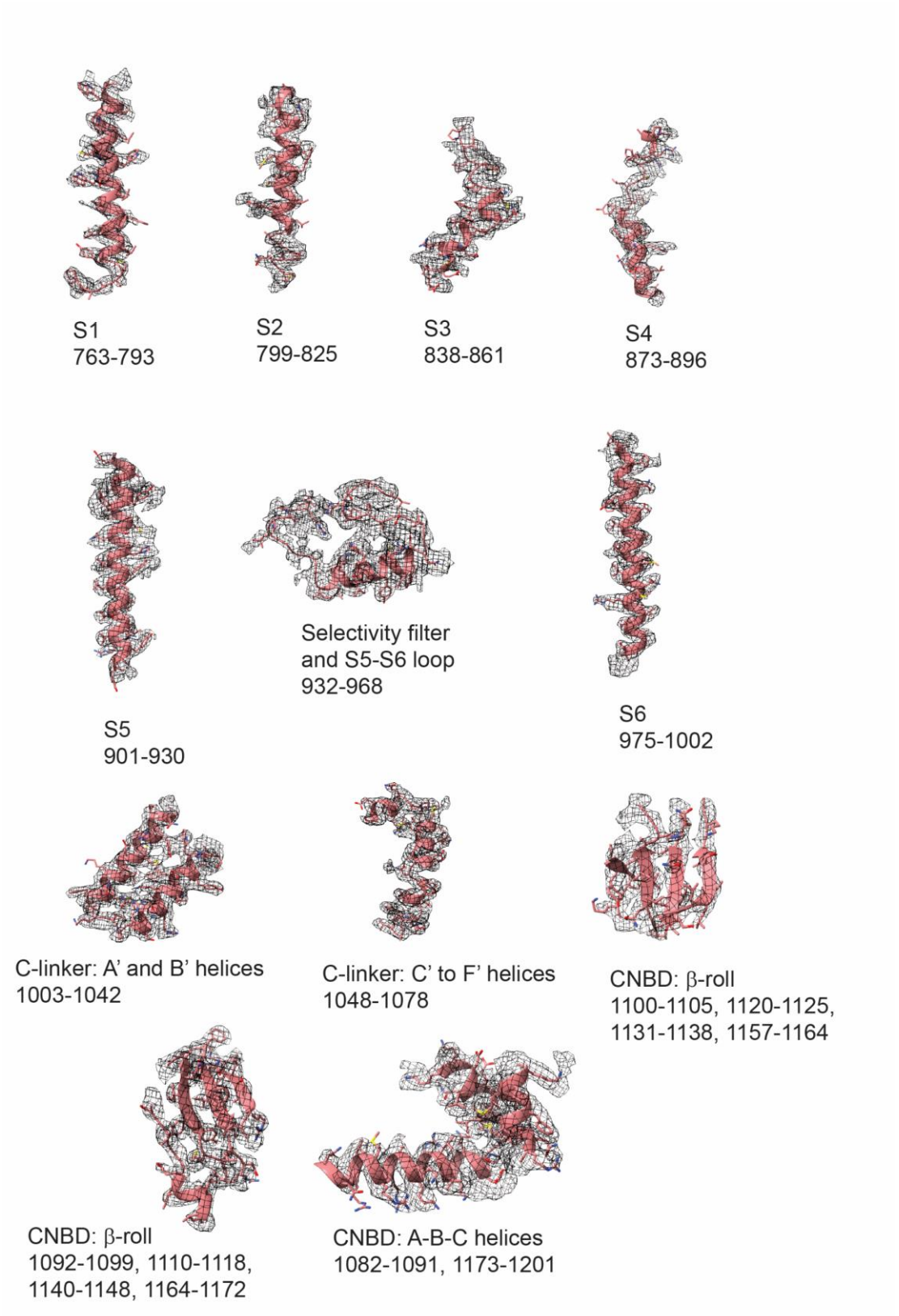

Figure S5. Cryo-EM density map of CNGB1 and relative atomic model of selected regions. The density map relative to the CNGB1 subunits (chain D) is shown. The map was contoured at threshold values ranging between 0.09 and 0.26 in ChimeraX.

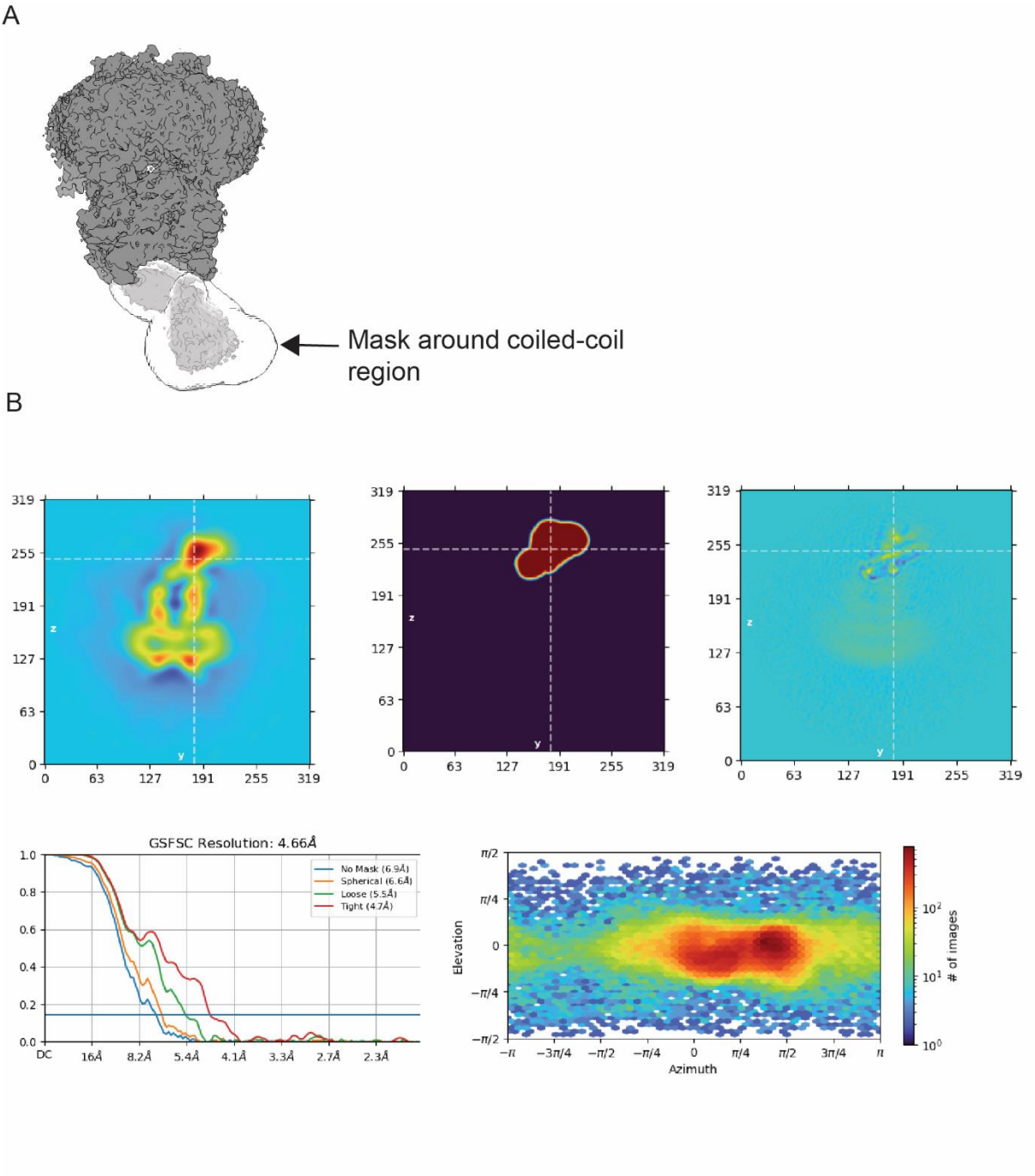

Figure S6. Details of the local refinement job with mask around the coiled-coil region. This local refinement job produced the density map shown in Fig. 2 of the main text. **A)** Overview of the mask used around the coiled-coil region. **B)** Output of the local refinement job in cryoSPARC.

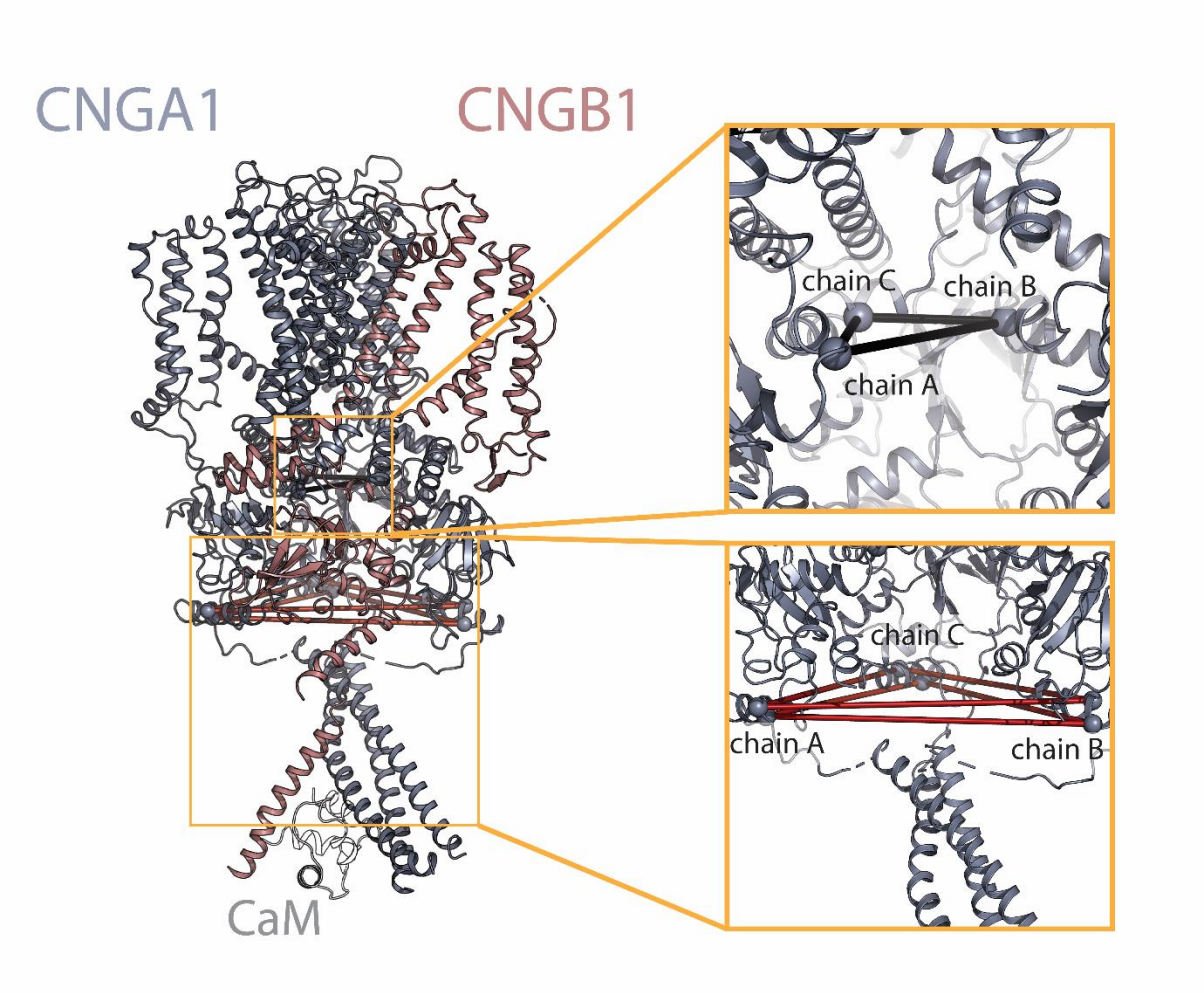

Figure S7: Identified Intermolecular selflinks on CNGA1.
Since the corresponding chains cannot be directly identified from the XL-MS data, all possible links are shown in the figure above. Satisfied links (< 30 Å, res 453 x 453) are shown in black. Violated links (res 596 x 596, res 598 x 598) are shown in red. As the violated crosslinks cannot be explained with our structure, they can probably be explained by a dimeric or an oligomeric structure of the CNG channel.

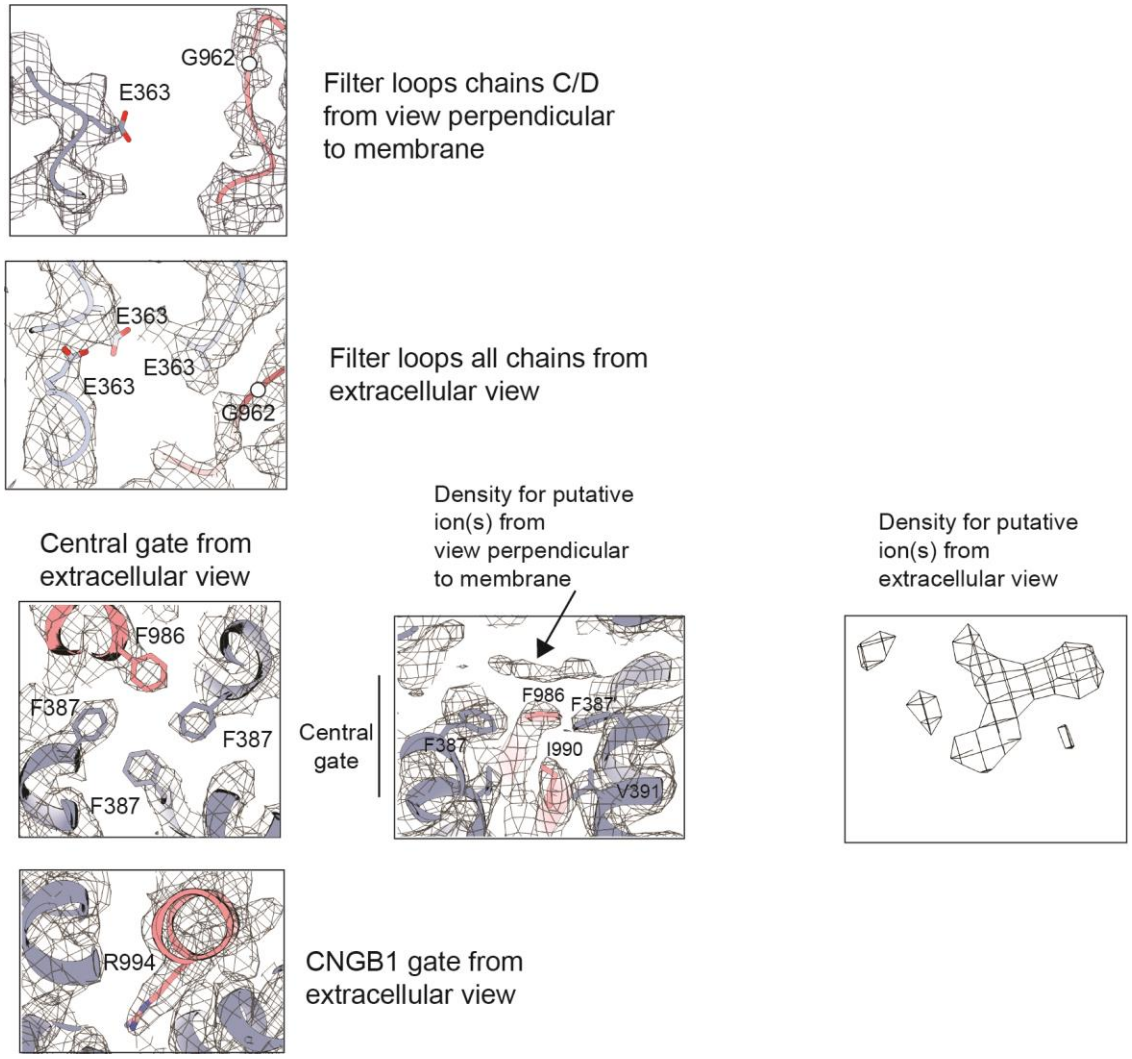

Figure S8. Details of the density map and model within the ion conduction pathway.

CNGA1:

Peptide	Region	Correlation	«EC_{50}» (nM added CaM)
TGYLEQGLLVKEER	219-232	0.93	2529
IDAIKQYMHFR	412-422	0.87	2440
YLPDKLR	454-460	0.87	3880
ESSVDLLQTR	629-638	0.98	78
SSVDLLQTR	630-638	0.99	223
VDLLQTR	632-638	0.97	162
PLIDTEF	666-672	0.92	516

CNGB1:

Peptide	Region	Correlation	«EC_{50}» (nM added CaM)
RWFEQNLEK	169-177	0.89	3116
GKGGEQESDAPVTC	274-287	0.87	4206
ASQNSAIINDR	671-681	0.97	44
SQNSAIINDR	672-681	0.93	33
QQQLLEQ	1261-1267	0.94	50

SI Table 2: Peptides grouped by their EC_{50} values.
All significantly changing peptides on CNGA1 and CNGB1, their corresponding correlations and EC_{50} values are shown above. Peptides highlighted in green show the lowest EC_{50} values, those are found on the CaM-binding domains (CaM1 and CaM2). Peptides highlighted in yellow are located on the coiled-coil region. The peptides with the highest EC_{50} values are kept in white.

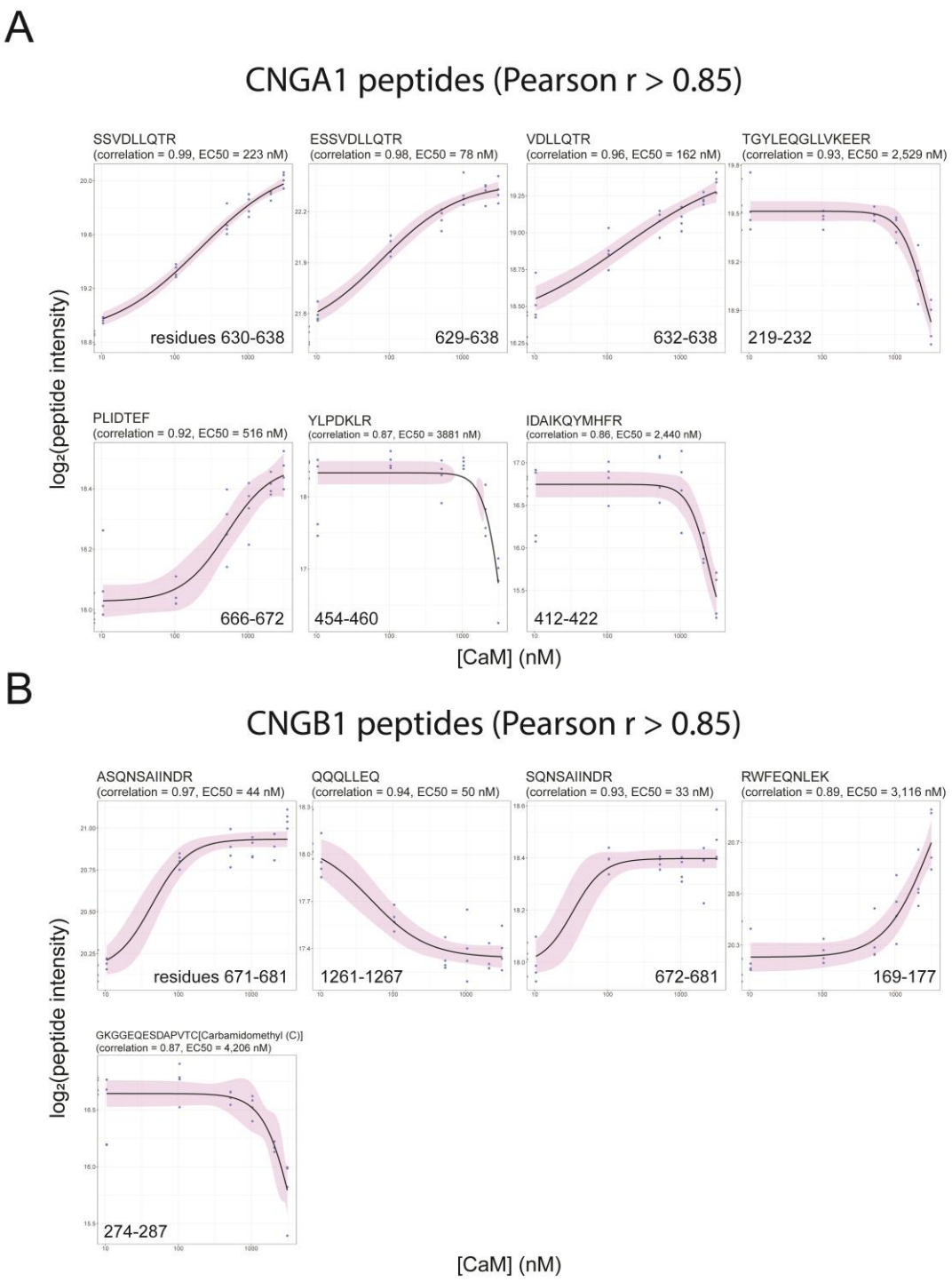

Figure S9. Significantly changing peptides on CNGA1 and CNGB1 sorted by their correlations

A) CNGA1 peptides with Pearson r > 0.85. **B)** CNGB1 peptides with Pearson r > 0.85. The peptide sequence, as well as their Pearson r (correlation) and EC50 values are mentioned in the title of each plot. The black line indicates the four-parameter dose-response model fit onto the measured peptide intensities. The log2 transformed peptide intensities for each replicate are shown as grey dots. The 95% model confidence interval is indicated as the pink shaded area.

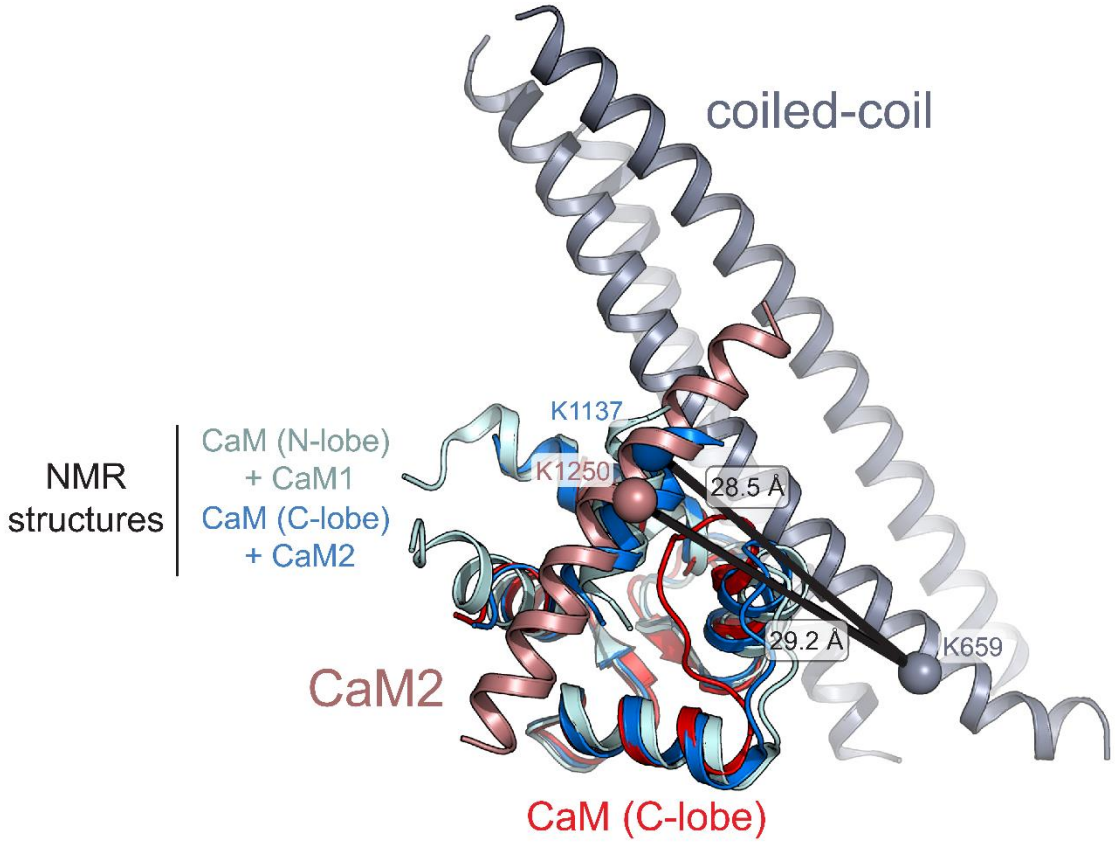

Figure S10. Aligned model of the coiled-coil domain (CNGA1) and CaM2 (CNGB1) with NMR structures of the CaM N-lobe with CaM1 and the CaM C-lobe with CaM2. Cryo-EM structures of the coiled coil domain (grey-blue), CaM2 (pink) and CaM (red) aligned with the NMR structures of the CaM C-lobe with CaM2 (blue; PDB: 8DGH; state 1) and the CaM N-lobe with CaM1 (pale green; PDB: 8DGK; state 1). Structures were aligned in PyMOL (align). The r.m.s.d. (root mean square deviation) for the aligned structures is 0.772 Å for the CaM N-lobe/CaM1 structure, and 1.137 Å for the CaM C-lobe/CaM2 structure. The measured distances of the identified crosslink between the coiled-coil domain and CaM2 (K659xK1250) and the equivalent distance for the NMR structures (K659xK1137) are indicated in boxes above the respective black lines.

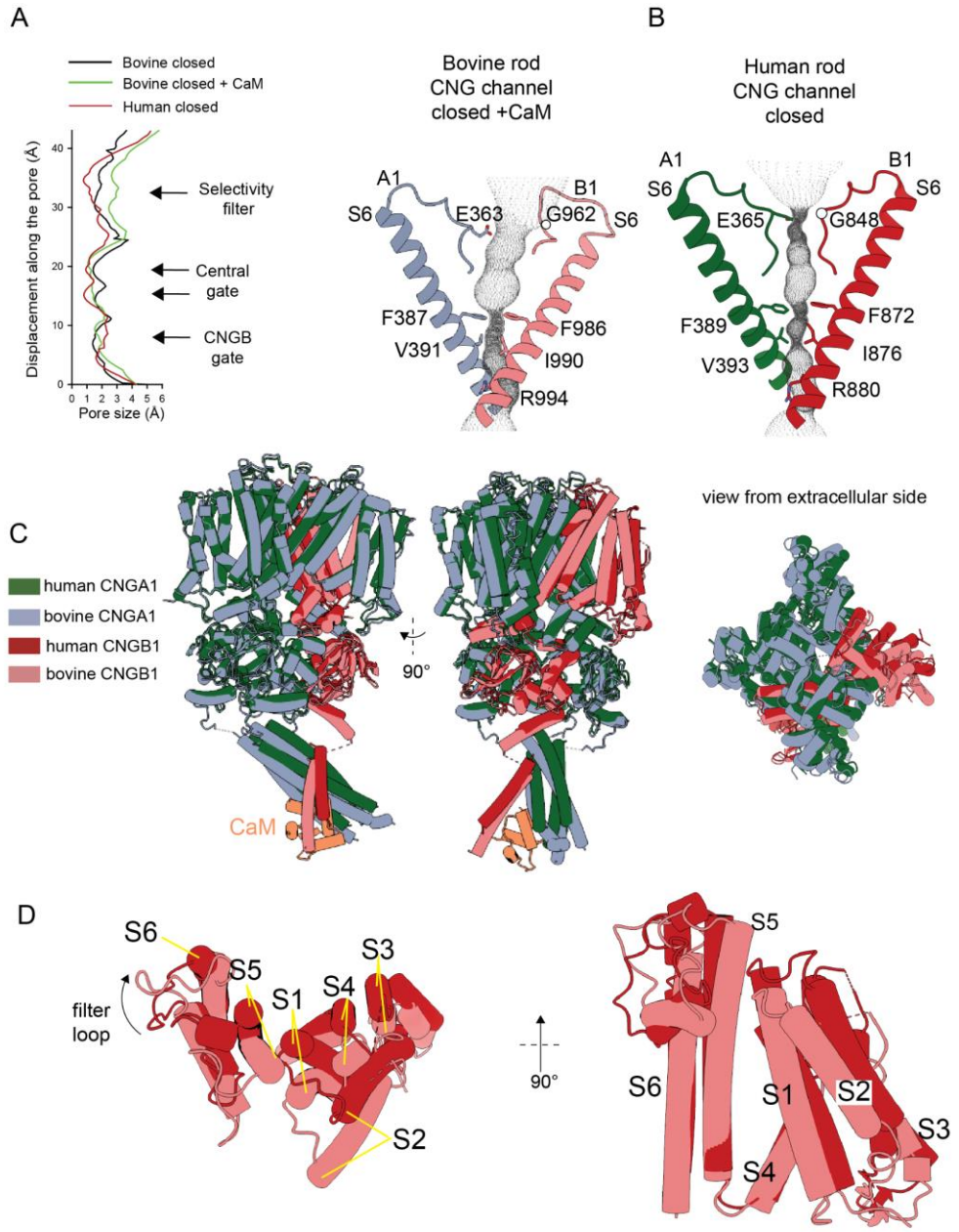

Figure S11. Comparison between the structures of the bovine and human rod CNG channel. A) Pore radius along the central axis calculated with HOLE [9] for the bovine structure without CaM (PDB: 7O4H), with CaM (this paper), the human rod channel in closed (PDB: 7RH9). In **B)** a side-to-side comparison of the pore of the bovine rod channel with CaM, and the human rod channel in closed state is shown (PDB: 7RH9). **C)** The superimposed structures of the bovine channel with CaM and the human channel in closed state with coiled-coil region (PDB: 7RHL). When superimposed in ChimeraX aligning the CNGB1 chains the r.m.s.d is 0.843 Å between 260 pruned atom pairs (across all 437 pairs: 4.183 Å). **D)** Details of the transmembrane regions of CNGB1 in the bovine structure with CaM, and in the human channel in closed state (PDB: 7RH9). Yellow lines indicate the different position of the transmembrane segments in the superimposed structures.

References:

1. Barret, D. C. A., Schertler, G. F. X., Benjamin Kaupp, U. & Marino, J. The structure of the native CNGA1/CNGB1 CNG channel from bovine retinal rods. *Nat. Struct. Mol. Biol.* **29**, 32–39 (2022).

2. Punjani, A., Rubinstein, J. L., Fleet, D. J. & Brubaker, M. A. cryoSPARC: algorithms for rapid unsupervised cryo-EM structure determination. *Nat. Methods* **14**, 290–296 (2017).

3. Emsley, P. & Cowtan, K. Coot: model-building tools for molecular graphics. *Acta Crystallogr. D. Biol. Crystallogr.* **60**, 2126–32 (2004).

4. Jumper, J. *et al.* Highly accurate protein structure prediction with AlphaFold. *Nature* **596**, 583–589 (2021).

5. Williams, C. J. *et al.* MolProbity: More and better reference data for improved all-atom structure validation. *Protein Sci.* **27**, 293–315 (2018).

6. Afonine, P. V. *et al.* Real-space refinement in PHENIX for cryo-EM and crystallography. *Acta Crystallogr. Sect. D Struct. Biol.* **74**, 531–544 (2018).

7. Pettersen, E. F. *et al.* UCSF ChimeraX: Structure visualization for researchers, educators, and developers. *Protein Sci.* **30**, 70–82 (2021).

8. *The PyMOL Molecular Graphics System, Version 1.2r3pre, Schrödinger, LLC.*

9. Smart, O. S., Neduvelil, J. G., Wang, X., Wallace, B. A. & Sansom, M. S. P. HOLE: A program for the analysis of the pore dimensions of ion channel structural models. *J. Mol. Graph.* **14**, 354–360 (1996).

10. Wessling-Resnick, M. & Johnson, G. L. Allosteric behavior in transducin activation mediated by rhodopsin. Initial rate analysis of guanine nucleotide exchange. *J. Biol. Chem.* **262**, 3697–3705 (1987).

11. Perez-Riverol, Y. *et al.* The PRIDE database resources in 2022: a hub for mass spectrometry-based proteomics evidences. *Nucleic Acids Res.* **50**, D543–D552 (2022).

12. Bruderer, R. *et al.* Extending the limits of quantitative proteome profiling with data-independent acquisition and application to acetaminophen-treated three-dimensional liver microtissues. *Mol. Cell. Proteomics* **14**, 1400–1410 (2015).

13. Cox, J. & Mann, M. MaxQuant enables high peptide identification rates, individualized p.p.b.-range mass accuracies and proteome-wide protein quantification. *Nat. Biotechnol.* **26**, 1367–1372 (2008).

14. Wickham, H. Welcome to the Tidyverse. *J. Open Source Softw.* **4**, 1686 (2019).

15. Dowle, M.; Srinivasan, A. data.table (v. 1.14.2). (2022).

16. Quast, J.P., Schuster, D., Picotti, P. protti: an R package for comprehensive data analysis of peptide- and protein-centric bottom-up proteomics data. *Bioinforma. Adv.* **2**, (2022).

17. Ritz, C., Baty, F., Streibig, J. C. & Gerhard, D. Dose-Response Analysis Using R. *PLoS One* **10**, e0146021 (2016).

18. UniProt: the universal protein knowledgebase in 2021. *Nucleic Acids Res.* **49**, D480–D489 (2021).

19. Leitner, A., Walzthoeni, T. & Aebersold, R. Lysine-specific chemical cross-linking of

protein complexes and identification of cross-linking sites using LC-MS/MS and the xQuest/xProphet software pipeline. *Nat. Protoc.* **9**, 120–137 (2014).

20. Combe, C. W., Fischer, L. & Rappsilber, J. xiNET: cross-link network maps with residue resolution. *Mol. Cell. Proteomics* **14**, 1137–1147 (2015).

21. Schiffrin, B., Radford, S. E., Brockwell, D. J. & Calabrese, A. N. PyXlinkViewer: A flexible tool for visualization of protein chemical crosslinking data within the PyMOL molecular graphics system. *Protein Sci.* **29**, 1851–1857 (2020).